J|A|C|S
ARTICLES
Published on Web 08/09/2003

# Modular and Tunable Chemosensor Scaffold for Divalent Zinc

Melissa D. Shults, Dierdre A. Pearce, and Barbara Imperiali*

*Contribution from the Department of Chemistry, Massachusetts Institute of Technology, Cambridge, Massachusetts 02139*

Received April 11, 2003; E-mail: imper@mit.edu

***Abstract:*** A modular peptide scaffold has been developed for fluorescent sensing of divalent zinc. The signaling component of the chemosensor is the chelation-sensitive fluorophore 8-hydroxy-5-(*N,N*-dimethylsulfonamido)-2-methylquinoline, which is prepared as the protected amino acid derivative Fmoc-Sox-OH and integrated into peptide sequences. Nineteen synthetic peptides incorporating the signaling element exhibit a range of affinities for $Zn^{2+}$ through variation of the type and number of $Zn^{2+}$ ligands, ligand arrangement and the $\beta$-turn sequence that acts as a preorganization element between the ligands. The stoichiometry of the peptide-$Zn^{2+}$ complexes is evaluated by several criteria. The fluorescence response of these peptides to pH and various important metal ions is reported. Eleven of these sequences form only 1:1 complexes with $Zn^{2+}$ and their affinities range from 10 nM to nearly 1 $\mu$M. When used in concert, these sensors can provide $Zn^{2+}$ concentration information in a valuable range.

## Introduction

Selective and tunable chemosensors for selected transition metal ions have the potential to afford qualitative and quantitative information about the presence, distribution and concentration of these metal ions in cells or tissues. Sensing divalent zinc is particularly desirable because of its physiological importance.[1] $Zn^{2+}$ is involved in cellular signaling pathways,[2] is implicated in signaling at neural synapses,[3] and is co-released with insulin from glucose-stimulated pancreatic islet $\beta$-cells.[4] A plethora of examples exist in the literature of intensity-based $Zn^{2+}$ fluorophore sensors,[5] from the earliest and widely used Zinquin and TSQ[6] to improved intensity probes such as ZPs,[7] ZnAFs,[8] FluoZin-3,[9] and those based on carbonic anhydrase.[10] The introduction of ratiometric ZnAF-R[11] and carbonic anhydrase-based[12] probes are also progress toward tools for determining $Zn^{2+}$ concentrations. Optimized sensors are still needed to quantify nanomolar to micromolar $Zn^{2+}$ concentrations. Previously, this laboratory has developed peptide-based $Zn^{2+}$ sensors[13−15] and we now report a new generation of smaller, more sensitive chemosensors with tuned affinity for divalent zinc in this range originating from the modular peptide architecture.

Quantifying free $Zn^{2+}$ is only possible at $Zn^{2+}$ concentrations at or near the dissociation constant of the chemosensor. Many of the currently available chemosensors are limited in that they either form 1:2 $Zn^{2+}$:chemosensor complexes[5] and/or that they have very tight affinities (sub nM).[7−9,11] Progress toward tuning selective $Zn^{2+}$ chemosensors for monitoring $Zn^{2+}$ at higher concentrations has been achieved but not without shortcomings. The dissociation constant of a dansylamide−polyamine macrocycle $Zn^{2+}$ sensor has been reduced to nearly 1 $\mu$M by altering the chelator moiety.[16] However, the $Zn^{2+}$ complexes of chemosensors containing aliphatic amine ligands exhibit significant competition with protons at physiological pH. Gee et al. have removed carboxylate ligands from $Ca^{2+}$ chemosensors to obtain several chemosensors with micromolar affinity for $Zn^{2+}$.[9b] These

(1) (a) Vallee, B. L.; Falchuk, K. H. *Physiol. Rev.* **1993**, *73*, 79−118. (b) Fraústo da Silva, J. J. R.; Williams, R. J. P. *The Biological Chemistry of the Elements: The Inorganic Chemistry of Life*, 2nd ed.; Oxford University Press: Oxford, 2001.
(2) Beyersmann, D.; Haase, H. *BioMetals* **2001**, *14*, 331−341.
(3) (a) Frederickson, C. J.; Bush, A. I. *BioMetals* **2001**, *14*, 353−366. (b) Frederickson, C. J.; Suh, S. W.; Silva, D.; Frederickson, C. J.; Thompson, R. B. *J. Nutr.* **2000**, *130*, 1471S−1483S. (c) Cuajungco, M. P.; Lees, G. J. *Neurobiol. Dis.* **1997**, *4*, 137−169.
(4) (a) Formby, B.; Schmid-Formby, F.; Grodsky, G. M. *Diabetes* **1984**, *33*, 229−234. (b) Grodsky, G. M.; Schmid-Formby, F. *Endocrinology* **1985**, *117*, 704−710.
(5) For reviews see: (a) Kimura, E.; Aoki, S. *BioMetals* **2001**, *14*, 191−204. (b) Burdette, S. C.; Lippard, S. J. *Coord. Chem. Rev.* **2001**, *216*, 333−361.
(6) See references within Canzoniero, L. M. T.; Sensi, S. L.; Choi, D. W. *Neurobiol. Dis.* **1997**, *4*, 275−279 and within ref 5a.
(7) (a) Walkup, G. K.; Burdette, S. C.; Lippard, S. J.; Tsien, R. Y. *J. Am. Chem. Soc.* **2000**, *122*, 5644−5645. (b) Burdette, S. C.; Walkup, G. K.; Spingler, B.; Tsien, R. Y.; Lippard, S. J. *J. Am. Chem. Soc.* **2001**, *123*, 7831−7841. (c) Burdette, S. C.; Frederickson, C. J.; Bu, W. M.; Lippard, S. J. *J. Am. Chem. Soc.* **2003**, *125*, 1778−1787.
(8) (a) Hirano, T.; Kikuchi, K.; Urano, Y.; Higuchi, T.; Nagano, T. *J. Am. Chem. Soc.* **2000**, *122*, 12 399−12 400. (b) Hirano, T.; Kikuchi, K.; Urano, Y.; Nagano, T. *J. Am. Chem. Soc.* **2002**, *124*, 6555−6562. (c) Ueno, S.; Tsukamoto, M.; Hirano, T.; Kikuchi, K.; Yamada, M. K.; Nishiyama, N.; Nagano, T.; Matsuki, N.; Ikegaya, Y. *J. Cell Biol.* **2002**, *158*, 215−220.
(9) (a) Gee, K. R.; Zhou, Z.-L.; Qian, W.-J.; Kennedy, R. *J. Am. Chem. Soc.* **2002**, *124*, 776−778. (b) Gee, K. R.; Zhou, Z.-L.; Ton-That, D.; Sensi, S. L.; Weiss, J. H. *Cell Calcium* **2002**, *31*, 245−251. (c) Qian, W.-J.; Gee, K. R.; Kennedy, R. T. *Anal. Chem.* **2003**, *75*, 3136−3143.
(10) (a) Fierke, C. A.; Thompson, R. B. *BioMetals* **2001**, *14*, 205−222. (b) Thompson, R. B.; Peterson, D.; Mahoney, W.; Cramer, M.; Maliwal, B. P.; Suh, S. W.; Frederickson, C.; Fierke, C.; Herman, P. *J. Neurosci. Methods* **2002**, *118*, 63−75.
(11) Maruyama, S.; Kikuchi, K.; Hirano, T.; Urano, Y.; Nagano, T. *J. Am. Chem. Soc.* **2002**, *124*, 10 650−10 651.
(12) Thompson, R. B.; Cramer, M. L.; Bozym, R.; Fierke, C. A. *J. Biomed. Optics* **2002**, *7*, 555−560.
(13) (a) Walkup, G. K.; Imperiali, B. *J. Am. Chem. Soc.* **1996**, *118*, 3053−3054. (b) Walkup, G. K.; Imperiali, B. *J. Am. Chem. Soc.* **1997**, *119*, 3443−3450.
(14) Walkup, G. K.; Imperiali, B. *J. Org. Chem.* **1998**, *63*, 6727−6731.
(15) Jotterand, N.; Pearce, D. A.; Imperiali, B. *J. Org. Chem.* **2001**, *66*, 3224−3228.
(16) Koike, T.; Abe, T.; Takahashi, M.; Ohtani, K.; Kimura, E.; Shiro, M. *J. Chem. Soc., Dalton Trans.*, **2002**, 1764−1768.

PET-chemosensors experience significant fluorescence in the absence of $Zn^{2+}$ due to incomplete PET quenching. Carbonic anhydrase-based $Zn^{2+}$ sensors have been developed to bind $Zn^{2+}$ with affinities over several orders of magnitude up to 1 $\mu$M.[10] Several variants of the carbonic anhydrase-based sensors have been developed for quantifying $Zn^{2+}$ via ratiometric, anisotropic or lifetime measurements on a single sensor; however, the sensors are large and suffer from the necessity of ternary complex formation.[10] Recently, a "reagentless" carbonic anhydrase-based sensor has been reported, which avoids ternary complex formation.[17] The goal of the research presented herein was to develop an addressable family of low molecular weight chemosensors with a range of $Zn^{2+}$ affinities, that can be used to determine $Zn^{2+}$ concentration via analysis of the relative intensities of the sensor readout.

A metal ion chemosensor built from a modular peptide scaffold offers many advantages. For example, the modular architecture enables implementation of any one of a number of fluorescence-based sensing mechanisms: chelation-enhanced fluorescence,[14,15] environment-sensitive fluorescence,[13] fluorescence quenching,[18] fluorescence resonance energy transfer,[19] and in some cases, metal-based fluorescence.[20] Additionally, both natural and nonnatural metal-binding amino acids can be integrated via combinatorial or design approaches, made facile via solid-phase peptide synthesis (SPPS). Binding optimization can be achieved by altering the type of ligands as well as their orientation and location within the peptide scaffold. Incorporation of other functionalities is also feasible via amide bond formation. For example, an additional fluorophore could be incorporated for ratiometric sensing, a cellular internalization sequence[21] could be appended to transport the sensors into cells, or the sensors could be attached to a solid support for diagnostic devices.

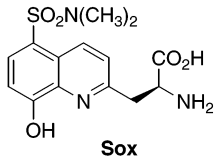


**Sox**

We have chosen to use chelation-enhanced fluorescence (CHEF) for sensing $Zn^{2+}$. In this mechanism, metal ion binding is accompanied by the generation of a new fluorescence emission signal. The fluorophore chosen for this purpose need not form a completely selective 1:1 complex with $Zn^{2+}$ because additional specificity determinants can be incorporated into the peptide sequence. Previously, we have reported that the quinoline derivative, 8-hydroxy-5-(*N*,*N*-dimethylsulfonamido)-2-methylquinoline, binds $Zn^{2+}$ and the complex has a much improved quantum yield over the parent fluorophore, 8-hydroxy-2-methylquinoline.[22] Integration of the enhanced CHEF fluorophore into the novel amino acid, Sox, and the design, synthesis, and evaluation of a family of chemosensors for $Zn^{2+}$ is reported.

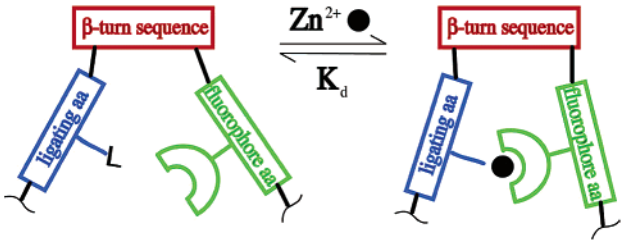


***Figure 1.*** Schematic representation of modular $Zn^{2+}$-binding peptides. To tune the $K_D$ for $Zn^{2+}$, the $\beta$-turn sequence, additional $Zn^{2+}$ ligand, and the ligand arrangement are altered.

The basic design of the chemosensor peptides includes a Sox residue and a residue that affords an additional ligand for $Zn^{2+}$ flanking a $\beta$-turn sequence, which pre-organizes the metal-ion binding site.[23] The necessity of a turn sequence for metal binding[23b] as well as its ability to tune affinity for the metal ion[23a] have been demonstrated previously. The basic features of the design are represented in Figure 1. To tune the affinity for $Zn^{2+}$, the additional ligand(s) for $Zn^{2+}$ and the $\beta$-turn sequence in the peptide are varied. Each peptide contains only six to eight amino acids. Two of these are serine residues, appended to the carboxy-terminus, to increase peptide solubility without interfering with metal binding. Further variation may be achieved through incorporation of an *N*-terminal module as a functionalized capping group instead of an amino acid derivative. Additional modules, of the types suggested earlier, may be incorporated at either terminus. Because the chemosensors reported herein are sufficiently polar not to be cell-permeable, they may be useful for detection of extracellular $Zn^{2+}$ or as a diagnostic tool for medical or environmental samples.

## Results and Discussion

**Synthesis of Fmoc-Sox-OH.** The synthesis of the protected amino acid is outlined in Scheme 1. The synthesis of **1** from 8-hydroxyquinaldine has been previously reported,[22] but the yield of the sulfonamide was improved by diluting the reaction mixture significantly. The phenolic hydroxyl group of **1** was then protected as the *tert*-butyldiphenylsilyl ether. The next three steps were performed without intermediate purification and include oxidation to the aldehyde with selenium dioxide, reduction to the alcohol with sodium borohydride, and bromination. Both the intermediate aldehyde and alcohol were unstable on silica gel. Purification of bromide **3** was accomplished via chromatography on florisil. This purified bromide contains 15% of **1** (by NMR) brought through from the selenium dioxide oxidation step. This impurity does not affect future reactions and can be washed away during peptide synthesis. Synthesis of the amino acid from **3** was performed by Corey's adaptation[24] of O'Donnell's asymmetric alkylation method,[25] utilizing (8S, 9R)-*O*-(9)-allyl-*N*-9-anthracenyl methylcinchonidium bromide as the phase-transfer catalyst. Because the benzophenone imine

(17) Thompson, R. B.; Maliwal, B. P.; Feliccia, V. L.; Fierke, C. A.; McCall, K. *Anal. Chem.* **1998**, *70*, 4717−4723.
(18) (a) Torrado, A.; Walkup, G. K.; Imperiali, B. *J. Am. Chem. Soc.* **1998**, *120*, 609−610. (b) Torrado, A.; Imperiali, B. *J. Org. Chem.* **1996**, *61*, 8940−8948.
(19) (a) Pearce, D. A.; Walkup, G. K.; Imperiali, B. *Bioorg. Med. Chem. Lett.* **1998**, *8*, 1963−1968. (b) Godwin, H. A.; Berg, J. M. *J. Am. Chem. Soc.* **1996**, *118*, 6514−6515.
(20) Franz, K.; Nitz, M.; Imperiali, B. *ChemBioChem* **2003**, *4*, 265−271.
(21) (a) Wadia, J. S.; Dowdy, S. F. *Curr. Opin. Biotech.* **2002**, *13*, 52−56. (b) Lindgren, M.; Hällbrink, M.; Prochiantz, A.; Langel, Ü. *Trends Pharmacol. Sci.* **2000**, *21*, 99−103.
(22) Pearce, D. A.; Jotterand, N.; Carrico, I. S.; Imperiali, B. *J. Am. Chem. Soc.* **2001**, *123*, 5160−5161.
(23) (a) Cheng, R. P.; Fisher, S. L.; Imperiali, B. *J. Am. Chem. Soc.* **1996**, *118*, 11 349−11 356. (b) Imperiali, B.; Kapoor, T. M. *Tetrahedron* **1993**, *49*, 3501−3510.
(24) (a) Corey, E. J.; Xu, F.; Noe, M. C. *J. Am. Chem. Soc.* **1997**, *119*, 12 414−12 415. (b) Corey, E. J.; Noe, M. C.; Xu, F. *Tetrahedron Lett.* **1998**, *39*, 5347−5350.
(25) O'Donnell, M. J. *Aldrichimica Acta* **2001**, *34*, 3−13.

***Scheme 1***

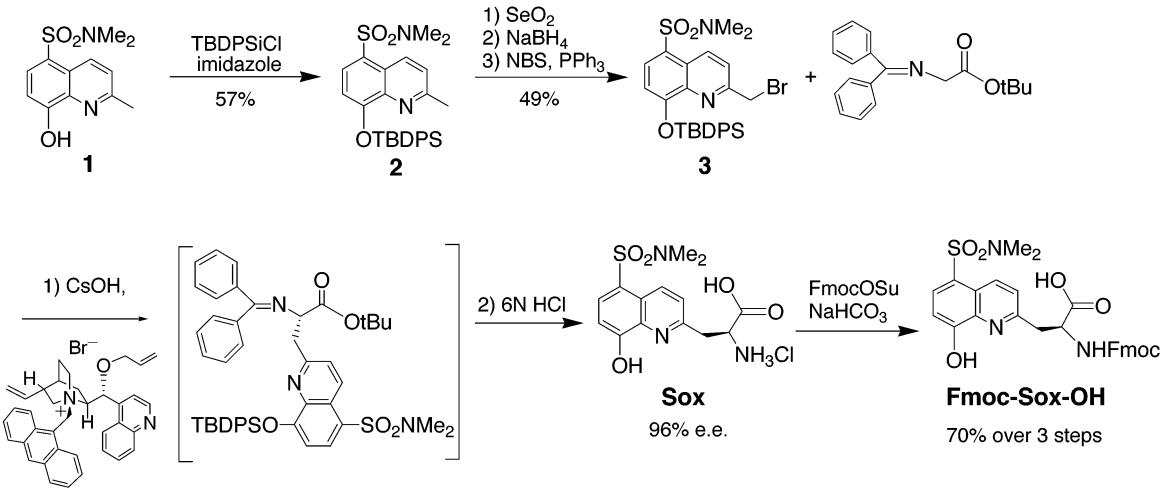


and *tert*-butyldiphenylsilyl ether are relatively acid labile, the adduct from the alkylation reaction was hydrolyzed in refluxing 6 N hydrochloric acid immediately upon completion of the alkylation. The product, Sox-OH, was isolated as the hydrochloride salt and used in the subsequent step without purification. A pure sample of this amino acid was derivatized with Marfey's reagent[26] to determine that the reaction gave 96% e.e. in favor of the L-enantiomer.[27] For subsequent peptide synthesis, the free amine was protected with the 9-fluorenyl-methoxycarbonyl (Fmoc) group by treatment with (9-fluorenylcarbonyl)succinimidyl carbonate (FmocOSu) to give Fmoc-Sox-OH (70% yield over 3 steps by NMR).

**Peptide Synthesis.** Fmoc-Sox-OH is used without purification in standard Fmoc SPPS. The small amount of peptide containing D-Sox was separated from the desired peptide during HPLC purification. The identity of each of the peptides was confirmed by mass spectrometry and purity was verified by RP-HPLC. Nineteen peptide sequences were designed and characterized (Table 1). The peptides differ in number and type of $Zn^{2+}$-binding ligands, ligand arrangement or $\beta$-turn sequence.

**Fluorescence Properties.** In the presence of saturating $ZnCl_2$, the Sox peptides exhibit a maximum emission at 500 nm with a maximum excitation at 360 nm. In addition, these peptides maintain the striking luminescence properties of the fluorophore.[22] The extinction coefficient and quantum yield values for representative chemosensor-$Zn^{2+}$ complexes were determined following quantitative amino acid analysis (QAA). These values are within 10% of 6200 $M^{-1}$ $cm^{-1}$ and 0.16, respectively.[28] In the absence of $Zn^{2+}$, the quantum yields are less than 0.005, indicating a 30-fold increase in fluorescence upon binding to $Zn^{2+}$.

**Summary of Binding Studies.** Peptide binding characteristics were assessed via titrations with $ZnCl_2$ and Job's plot analysis to determine the affinity and stoichiometry of complex formation. Titration data is fit with the program Specfit/32,[29] which analyzes multiwavelength data using an iterative method to obtain the association constant in terms of the free (unbound) $Zn^{2+}$ concentration, $[Zn^{2+}]_f$. Direct titrations were performed for all peptide sequences under similar conditions for comparison purposes. Buffered $Zn^{2+}$ solutions have been used for other tighter-binding $Zn^{2+}$ chemosensors and require only certain buffer and ionic strength conditions where the binding constant of a $Zn^{2+}$ chelator has been previously determined.[7−9,11] Only

***Table 1.*** Dissociation Constants for $Zn^{2+}$ Peptidyl Chemosensors

| No. | Peptide Sequence | Apparent $K_D$ for 1:1 complex (nM)[a] | Complex(es) formed |
|---|---|---|---|
| P1 | Ac-Sox- Pro-DSer- Pen-Ser-Ser-$NH_2$[b] | 9.6 ± 2.6 | 1:1 |
| P2 | Ipa-Gly-Cys-DPro-Gly- Sox-Ser-Ser-$NH_2$[c] | 11 ± 2 | 1:1 |
| P3 | Ac-Sox- Pro- Gly- Cys-Ser-Ser-$NH_2$ | 12 ± 1 | 1:1 |
| P4 | Ac-Cys- Pro-DSer- Sox-Ser-Ser-$NH_2$ | 15 ± 4 | 1:1 |
| P5 | Ac-Sox- Pro-DSer- Cys-Ser-Ser-$NH_2$ | 19 ± 5 | 1:1 |
| P6 | Ipa-Gly-His-DPro-Ser- Sox-Ser-Ser-$NH_2$[e] | 35 ± 5 | 1:1 |
| P7 | Ac-Sox- Pro-DSer- pSer-Ser-Ser-$NH_2$[d] | 130 ± 10 | 1:1 |
| P8 | Ac-Sox- Pro-DSer- His-Ser-Ser-$NH_2$ | 190 | 1:1, 1:2 |
| P9 | Ipa- Pro-βPhe- Sox-Ser-Ser-$NH_2$[c,e] | 330 | 1:1, 1:2 |
| P10 | Ipa- DPro-Gly- Sox-Ser-Ser-$NH_2$[e] | 360 ± 20 | 1:1 |
| P11 | Ipa- DPro-Ser- Sox-Ser-Ser-$NH_2$[e] | 530 ± 30 | 1:1 |
| P12 | Ac-Sox- Pro-DSer- Glu-Ser-Ser-$NH_2$ | 730 ± 80 | 1:1 |
| P13 | Ac-Sox- Pro-DSer- Asp-Ser-Ser-$NH_2$ | 910 ± 50 | 1:1 |
| P14 | Ipa- Pro- Gly- Sox-Ser-Ser-$NH_2$[c] | 990 | 1:1, 1:2 |
| P15 | Ipa- Pro-DSer- Sox-Ser-Ser-$NH_2$[e] | 1100 | 1:1, 1:2 |
| P16 | Ipa- Gly-Asn- Sox-Ser-Ser-$NH_2$[c] | 1600 | 1:1, 1:2 |
| P17 | Ipa- Pro- Ser- Sox-Ser-Ser-$NH_2$[e] | 1900 | 1:1, 1:2 |
| P18 | Ipa- Pro-βPhe- Sox-Ser-Ser-$NH_2$[c,e] | 3000 | 1:1, 1:2 |
| P19 | Ac-Sox- Pro-DSer- Phe-Ser-Ser-$NH_2$ | 12000 | 1:1, 1:2 |

[a] Obtained via direct fluorescence titration. Values reported with standard deviation are obtained from triplicate titrations with a peptide concentration near the $K_D$. Values without standard deviations are obtained via a single titration at [peptide] = 50 nM. $K_D$ values are calculated by a global nonlinear least-squares fit with the program Specfit/32.[29] [b] Pen = $\beta$-dimethylcysteine. [c] Ipa = 3-(imidazol-4-yl)propionic acid. [d] pSer = phosphoserine. [e] $\beta$Phe = 3-amino-3-phenylpropionic acid. P9 and P18 each contain one of the enantiomers of DL-$\beta$Phe.

(26) Fujii, K.; Ikai, Y.; Mayumi, T.; Oka, H.; Suzuki, M.; Harada, K. *Anal. Chem.* **1997**, *69*, 3346−3352.
(27) The preference for L-enantiomer formation with the catalyst *O*-(9)-allyl-*N*-9-anthracenyl methylcinchonidium bromide is well-established over a wide range of electrophiles. See refs 24 and 25.
(28) Some variation between peptide sequences in the extinction coefficients was observed due to the error associated with the stock solution concentration determined by QAA. The error in this measurement is at least 10%. The values are detailed in the Supporting Information.
(29) SPECFIT/32 for Windows (version 3.0), Spectrum Software Associates, Marlborough, MA.

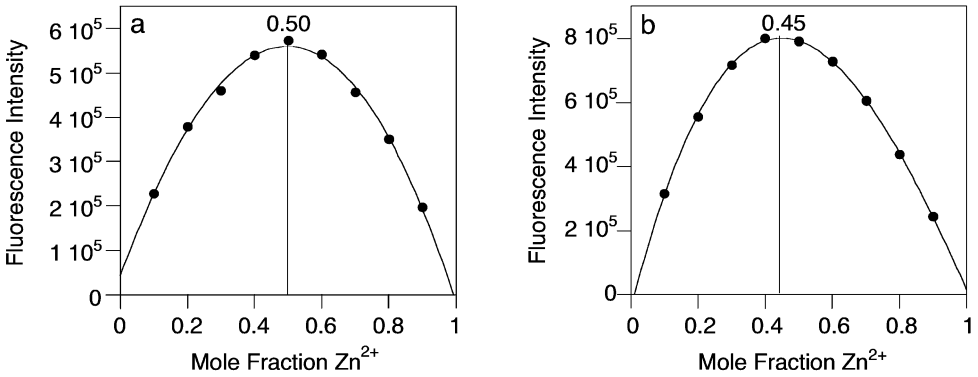


***Figure 2.*** Job plots for (a) P13 (forms only 1:1 complexes) and (b) P8 (forms both 1:1 and 1:2 complexes). The total [peptide] + [$ZnCl_2$] = 0.98 $\mu$M.

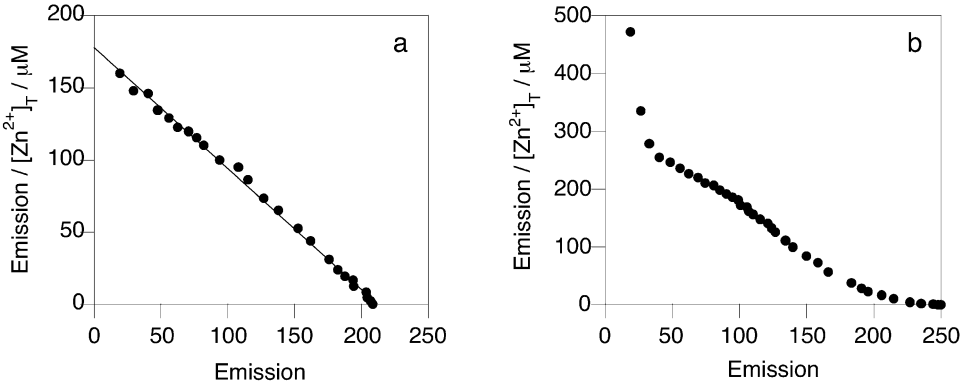


***Figure 3.*** Scatchard plots for (a) P13 and (b) P8. Titrations were performed with 500 nM peptide. Data for entire titration is included.

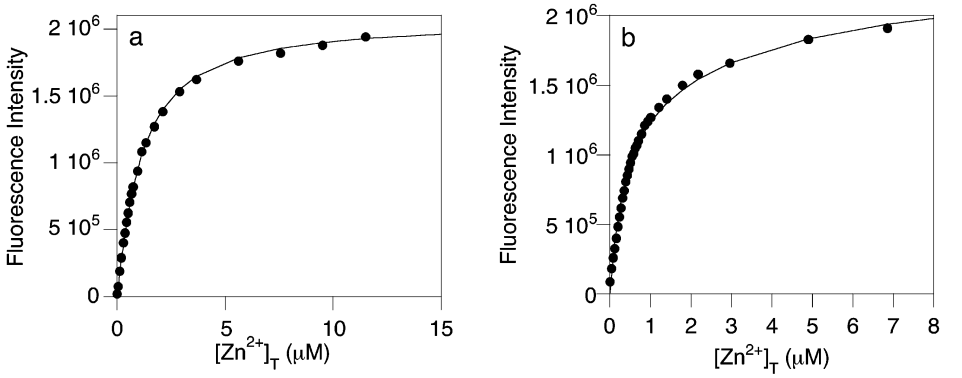


***Figure 4.*** Fit obtained from titration data for (a) P13 using a 1:1 complexation model and (b) P8 using a 1:1 and 1:2 complexation model. With these models specified, a global nonlinear least-squares fit of the data was obtained via Specfit/32.[29]

the 1:1 complex dissociation constants are listed in Table 1 and discussed in the following section because these depend the most heavily on the $\beta$-turn sequence and the additional $Zn^{2+}$ ligand.

**Binding Stoichiometry.** For the peptides in Table 1, four criteria were evaluated to determine binding stoichiometry: a Job's plot analysis, a Scatchard plot, the model used for $K_D$ calculation and the maximum fluorescence emission wavelength. To illustrate the conclusion from each method, data for peptides P8 and P13 are included. These data are representative of all peptide sequences synthesized. A Job's plot[30] that is symmetrical and exhibits a maximum at 0.5 mole fraction of $Zn^{2+}$ indicates that only a 1:1 complex is formed (Figure 2a). However, a Job's plot with a maximum at any other value besides 0.5 indicates more complex equilibria (Figure 2b).[30] A Scatchard plot of extracted titration data at a single wavelength is linear only for peptides forming solely a 1:1 complex (Figure 3).[30] Peptides forming a 1:1 complex exclusively throughout the course of a titration obtain a better fit with a 1:1 complexation model (Figure 4). Addition of a 1:2 $Zn^{2+}$:peptide complex into the model fits the data for all other peptides. Additionally, the wavelength of maximum emission for a peptide forming only a 1:1 complex remains constant at 500 nm during the course of a titration (Figure 5a). On the other hand, peptides forming 1:1 and 1:2 complexes exhibit shifts in the maximum emission wavelength from 475 to 500 nm as increasing amounts of $Zn^{2+}$ are added (Figure 5b). This shift is seen because the 1:2 complex is also fluorescent.

For some sequences, an increase of peptide concentration increases the likelihood for 1:2 complex formation because any two given peptides are in closer proximity. The rigid imidazole

(30) Connors, K. A. *Binding Constants: The Measurement of Molecular Complex Stability*; John Wiley and Sons: New York, 1987.

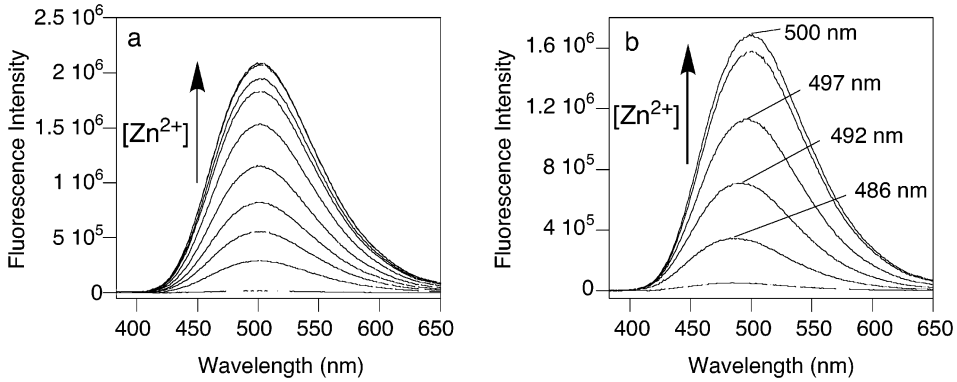


***Figure 5.*** Spectra recorded for the titration of (a) P13 (emission maximum remains constant at 500 nm) and (b) P8 (emission maximum shifts during the titration). Only a few of the 25 spectra collected are shown for clarity.

***Table 2.*** Dissociation Constants for 1:1 $Zn^{2+}$:Peptide Complexes

| | $Zn^{2+}$ ligands (N → C) | Turn | Apparent $K_D$[a] (nM) |
|---|---|---|---|
| P1 | Sox, Pen | Pro-D-Ser | 9.6 ± 2.6 |
| P2 | Ipa, Cys, Sox | D-Pro-Gly | 11 ± 2 |
| P3 | Sox, Cys | Pro-Gly | 12 ± 1 |
| P4 | Cys, Sox | Pro-D-Ser | 15 ± 4 |
| P5 | Sox, Cys | Pro-D-Ser | 19 ± 5 |
| P6 | Ipa, His, Sox | D-Pro-Ser | 35 ± 5 |
| P7 | Sox, pSer | Pro-D-Ser | 130 ± 10 |
| P10 | Ipa, Sox | D-Pro-Gly | 360 ± 20 |
| P11 | Ipa, Sox | D-Pro-Ser | 530 ± 30 |
| P12 | Sox, Glu | Pro-D-Ser | 730 ± 80 |
| P13 | Sox, Asp | Pro-D-Ser | 910 ± 50 |

[a] Obtained via direct fluorescence titration in triplicate. $K_D$ values are calculated by a global nonlinear least-squares fit with the program Specfit/32.

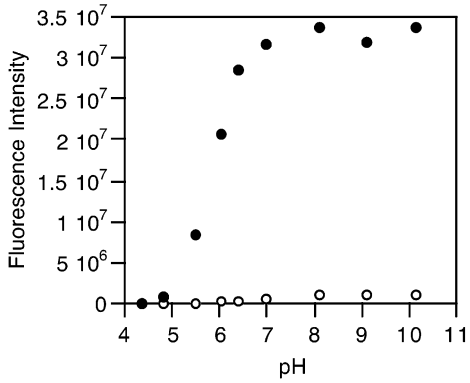


***Figure 6.*** pH dependence of fluorescence intensity for P10 (open circles) and the P10−$Zn^{2+}$ complex (closed circles).

ligand was more sensitive to modification of the turn sequence and the ligand arrangement; not all peptides synthesized with this ligand formed only 1:1 complexes. With the exception of P8, P15, P18, and P19, all peptides form only the 1:1 complex at peptide concentrations of 50 nM. Many peptide sequences form more favorable 1:1 complexes, indicated by their preference for 1:1 complex formation at higher peptide concentrations.

Of the nineteen peptides synthesized, eleven form 1:1 complexes in a useful range for biological experiments (low micromolar). Only these peptides (Table 2) will be further discussed, as they are the most useful. For peptides that form mixed complexes, determination of $Zn^{2+}$ concentrations is complicated by the fact that relative concentrations of the 1:1 and 1:2 complexes change depending on peptide concentration and $Zn^{2+}$ concentration.

**Binding Trends.** Inspection of the data presented in Table 2 allows the conclusion that the nonfluorophore $Zn^{2+}$ ligands provide rough tuning of binding affinity. A peptide's affinity for $Zn^{2+}$ decreases along the following series: thiolate > two imidazoles > phosphate > one imidazole > carboxylate. This trend is expected based on the binding preferences of the $Zn^{2+}$ ion, where "softer" ligands are preferred.[1,31] The affinity of these peptides for $Zn^{2+}$ spans 2 orders of magnitude through ligand variation. Fine-tuning of binding affinity was possible through modification of the turn sequence and ligand arrangement. In general, a more flexible Gly in the turn sequence leads to a slightly tighter-binding peptide. In addition, incorporation of two imidazole ligands greatly increased the affinity over one imidazole ligand, but the addition of an imidazole ligand to a cysteine-containing peptide barely changed the affinity.

**Implications for Further Tuning.** The possibility of additional $Zn^{2+}$ chemosensors with altered affinities is feasible through continued modification of this architecture considering the following trends. In general, affinity can be increased with softer ligands, a more flexible turn, and additional ligands. Affinity can be weakened with harder ligands and increased turn rigidity. Synthesis and characterization of the new chemosensor must be the final and necessary step to confirm the utility of each new design.

**Competition Studies.** To evaluate the potential utility of these sensors, the influence of protons and metal ions on the ability of the chemosensor to sense $Zn^{2+}$ was investigated. Two separate experiments were performed to assess possible interference on the detection of $Zn^{2+}$: one to assess false positive responses where the competing entity forms a fluorescence complex with the chemosensor and another to identify false negative responses where the ability of the sensor to bind $Zn^{2+}$ is compromised.

The fluorescence of each peptide in the absence of $Zn^{2+}$ remains essentially unchanged between pH 4 and 10, whereas the fluorescence of each peptide-$Zn^{2+}$ complex is quenched below pH 5. All of the peptide-$Zn^{2+}$ complexes are maximally fluorescent at and above pH 7. Figure 6 shows the fluorescence intensity of P10 and the P10−$Zn^{2+}$ complex as a function of

(31) The phosphate ligand appears out of order if solely a "soft" ligand explanation is invoked to explain increased $Zn^{2+}$ affinity. The increased affinity of P7 for $Zn^{2+}$ relative to the "softer" imidazole ligand may be due to its increased negative charge and/or its ability to bind as a bidentate ligand.

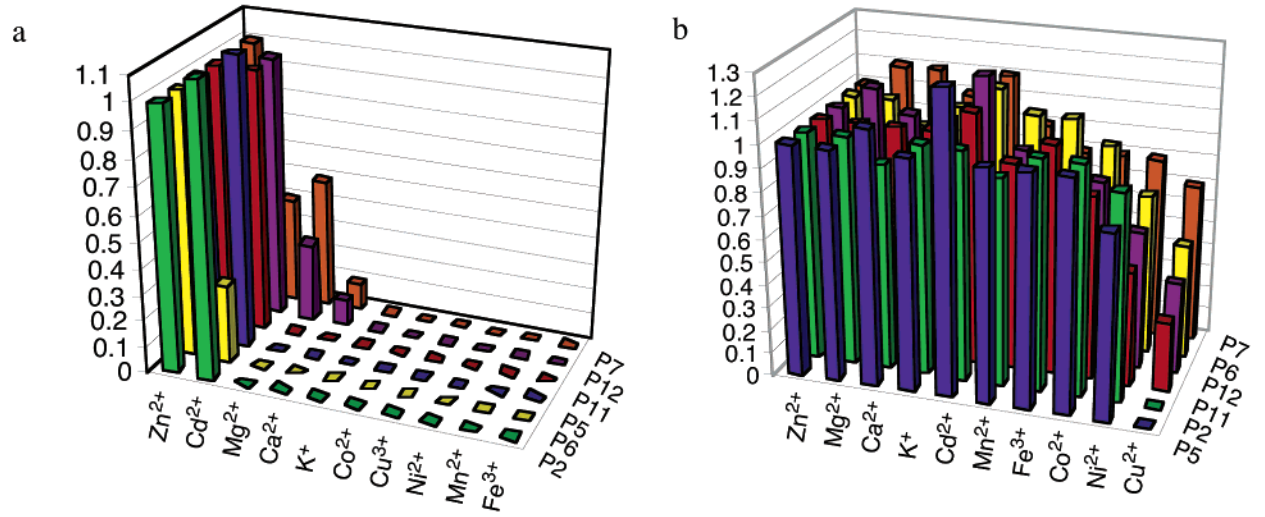


***Figure 7.*** Metal ion competition plots for representative peptide sequences, based on donor ligands. (a) Fluorescence intensity of peptides in the presence of various cations. (b) Fluorescence intensity of peptide plus 1 equivalent of $Zn^{2+}$ in the presence of various cations. All metal ions were evaluated at one equivalent except $Ca^{2+}$, $Mg^{2+}$ and $K^{+}$ which were used at 1 mM. Peptide concentrations were either 1 $\mu$M (P2, P5, P6 and P7) or 10 $\mu$M (P11, P12).

pH. This plot is representative of all peptide sequences; the pH profiles differ only very slightly due to the ligand variation.

In general, the metal ion response variation between peptides can be explained as due to donor-atom preference for each metal ion.

The fluorescence response of each sensor in the presence of each metal cation was investigated (Figure 7a), since metal ions besides $Zn^{2+}$ are known to form fluorescent complexes with 8-hydroxyquinoline, including $Mg^{2+}$ and $Ca^{2+}$.[32] Only peptides containing "hard" carboxylate and phosphate donor ligands (P7, P12, P13) give a response with 1 mM $Mg^{2+}$ and $Ca^{2+}$. The response to $Mg^{2+}$ is greater likely because the size of $Mg^{2+}$ is more comparable to $Zn^{2+}$ than that of $Ca^{2+}$.[1b] P7 gives a substantial response to $Mg^{2+}$ (50%) because $Mg^{2+}$ has a particularly high affinity for phosphate, as seen by its frequent coordination to phosphate ligands in ATP and oligonucleotide sequences.[1b] Further details concerning $Mg^{2+}$ and $Ca^{2+}$ binding to P7, P12, and P13 can be found in the Supporting Information.

Because many other metal ions do not form fluorescent complexes with 8-hydroxyquinoline, the fluorescence response of the peptide-$Zn^{2+}$ complex in the presence of 1 equivalent of several additional metal ions was investigated (Figure 7b). $K^{+}$ does not interfere with fluorescence for any peptide-$Zn^{2+}$ complex up to 1 mM. For weaker $Zn^{2+}$-binding peptides, $Mn^{2+}$ and $Co^{2+}$ compete with $Zn^{2+}$ binding by no more than 10% and 20%, respectively. $Fe^{3+}$ interferes for peptides with "hard" oxygen donor atoms (P7, P12, P13). $Ni^{2+}$ causes significant quenching for peptides with imidazole and carboxylate ligands but has little affinity for peptides with thiolate and phosphate ligands. $Cu^{2+}$ interferes with $Zn^{2+}$ binding for all peptides, and it entirely competes with $Zn^{2+}$ for peptides containing thiolate ligands (P1, P2, P5).

With the exception of $Ca^{2+}$, $Mg^{2+}$, and $K^{+}$, all metal ions investigated are unlikely to be present as the free metal ion in biological systems. Regulatory proteins which bind $Cu^{2+}$ and $Zn^{2+}$ ions sufficiently tightly to preclude the possibility of free amounts of these metals in the cytoplasm have been discovered and most likely, similar regulatory proteins for other metal ions exist.[33,34] For diagnostic purposes, a sensor can be chosen based on its lack of response to a competing metal ion in addition to its dissociation constant.

In addition, these chemosensors all form fluorescent complexes with $Cd^{2+}$. The concentration of $Cd^{2+}$ in biological systems is typically very low[1b] and thus is unlikely to interfere with measurements in such systems. However, environmental and diagnostic applications exist for a $Cd^{2+}$ chemosensor due to the toxicity of this metal ion. $Cd^{2+}$ forms complexes that are as fluorescent as the ones with $Zn^{2+}$ for all peptides, but does not bind as effectively to peptides P6 and P7 as $Zn^{2+}$. Sensors are rarely able to differentiate between $Zn^{2+}$ and $Cd^{2+}$. It is likely that $Cd^{2+}$ is too large to efficiently bind to all four ligands of P6. In addition, $Cd^{2+}$ is considered an even "softer" metal ion than $Zn^{2+}$ and has less affinity for phosphate ligands than $Zn^{2+}$ in P7. These trends imply that the peptide scaffold could be tuned for the specific detection of $Cd^{2+}$ as well.

**Probes of $Zn^{2+}$ Concentration.** For a given application, peptides spanning the range of affinities may be selected for an experiment and the $Zn^{2+}$ concentration can be determined within a defined range where one sensor gives a fluorescent response when another does not. To illustrate this, vials with different probes and varying amounts of $Zn^{2+}$ were prepared (Figure 8). The fluorescence of each peptide at each of the three concentrations corresponds well with the data obtained from titrations. $Zn^{2+}$ concentrations can be narrowed into a range based on the responses of two or more peptides. This measurement does not require that the maximal fluorescence intensity be known, but only that one peptide does not give a response. This method avoids many of the well-known difficulties associated with intensity-based measurements because the chemosensors are sufficiently similar to be compared under identical experimental conditions. For example, a solution that fluoresces in the presence of P5 but does not fluoresce in the presence of P7 would contain a $Zn^{2+}$ concentration between roughly 50 and 200 nM. Only very simple illumination equipment is required.

(32) Seitz, W. R. *CRC Critical Reviews in Analytical Chemistry*; CRC Press: Boca Raton, FL, 1980; pp 367−404.
(33) Outten, C. E.; O'Halloran, T. V. *Science* **2001**, *292*, 2488−2492.
(34) Rae, T. D.; Schmidt, P. J.; Pufahl, R. A.; Culotta, V. C.; O'Halloran, T. V. *Science* **1999**, *284*, 805−808.

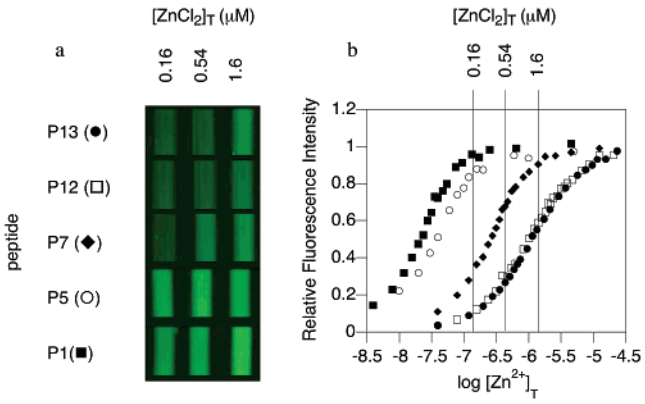


***Figure 8.*** (a) Visual representation of the range of $Zn^{2+}$ affinities of five of the peptides. Vials were loaded with a 1 $\mu$M solution of the appropriate peptide in 50 mM HEPES buffer at pH 7 containing 150 mM NaCl and the indicated concentration of $ZnCl_2$. Vials were irradiated at 365 nm on a UV transilluminator. (b) Comparison of the fluorescence responses in (a) with the titration curves shows the probes behave as expected.

## Conclusion

In conclusion, a nonnatural amino acid Sox has been synthesized and used as a modular building block in peptide sequences that bind $Zn^{2+}$ in the nanomolar to micromolar range, where few useful $Zn^{2+}$ chemosensors currently exist. The affinity for $Zn^{2+}$ was tuned by variation of the ligands, scaffold, and turn sequence of the peptide. Eleven peptide sequences that bind to $Zn^{2+}$ in a 1:1 complex with affinities spanning 10 nM to 1 $\mu$M are summarized in Table 2. The general trends gleaned from the binding constants reported have implications for further tuning to generate new sensors. Competition analysis with protons and important metal ions show these probes to be sufficiently selective for $Zn^{2+}$ under conditions for biological and diagnostic experiments. Chemosensors from this family can be chosen for applications based on their $Zn^{2+}$-affinity as well as their metal ion preferences. The sensors can be used easily to determine $Zn^{2+}$ concentration when one sensor gives a positive response and another does not. For $Zn^{2+}$ concentration determination with a single sensor, investigation of ratiometric $Zn^{2+}$ sensors based on this scaffold are in progress.

**Acknowledgment.** Research grants from the NSF (CHE-9996335) and an NSF graduate research fellowship for M.D.S. are gratefully acknowledged. The NMR spectrometers at MIT were provided by grants from the NSF (DBI-9729592 and CHE-9808061) and NIH (1S10RR13886-01). M.D.S. would like to thank Dr. N. Jotterand for early procedures toward the synthesis of the amino acid, Dr. K. J. Franz for helpful discussions and Dr. R. A. Binstead of Spectrum Software Associates for assistance with the Specfit/32 program.

**Supporting Information Available:** Synthetic procedures and characterization for Sox and peptides, $^1H$ NMR spectra of 2, 3, Sox, and Fmoc-Sox-OH, experimental details for all fluorescence experiments (PDF). This material is available free of charge via the Internet at http://pubs.acs.org.

JA0355980